Original Article

Predicting recurrent laryngeal nerve invasion by preoperative ultrasonography in patients with thyroid carcinoma

Yushuang He[1], Yujia Yang[1], Wen Wen[1], Li Qiu[1], Zhihui Li[2], Jianyong Lei[2]

[1]Department of Ultrasound, West China Hospital of Sichuan University, Chengdu, China; [2]Department of Thyroid Surgery, West China Hospital of Sichuan University, Chengdu, China

Contributions: (I) Conception and design: All authors; (II) Administrative support: L Qiu, Z Li; (III) Provision of study materials or patients: Y He, L Qiu, Z Li, J Lei; (IV) Collection and assembly of data: Y He, Y Yang; (V) Data analysis and interpretation: Y He, W Wen; (VI) Manuscript writing: All authors; (VII) Final approval of manuscript: All authors.

Correspondence to: Li Qiu, PhD. Department of Ultrasound, West China Hospital of Sichuan University, #37 Guoxue Alley, Chengdu 610041, China. Email: qiulihx@scu.edu.cn; Zhihui Li, PhD. Department of Thyroid Surgery, West China Hospital of Sichuan University, #37 Guoxue Alley, Chengdu 610041, China. Email: rockoliver@vip.sina.com.

Background: For thyroid cancer staging, evaluation of extent of local invasion, including recurrent laryngeal nerve (RLN), may assist surgical decision-making.

Methods: This prospective study evaluated patients who underwent thyroidectomy at a single tertiary-level academic institution. Patients with complete clinical information and ultrasound imaging of thyroid carcinoma and RLN were enrolled. Those who had thyroidectomy before or did not fit the above conditions were excluded. Patients were assigned to either a development or validation cohort. Development of models was constructed in a primary cohort based on preoperative ultrasound features and clinicodemographic data from August 2020 to December 2021. Validation of the models was then performed on an independent cohort between January and March of 2022. Multivariate logistic regression and nomograms were mainly used for statistical analysis.

Results: Using data from 816 patients (80 RLN invasion), we built nomogram 1 based on age [95% confidence interval (CI): 1.315 to 145.933, P=0.029], body mass index (BMI; 95% CI: 1.228 to 10.874, P=0.020), tumor size (95% CI: 4.677 to 1,373.1, P=0.002), tumor adjacent to medial (95% CI: 1.816 to 26.713, P=0.005) and posterior thyroid capsules (95% CI: 5.567 to 756.583, P=0.001), and distance <1 mm between tumor and the RLN (95% CI: 10.389 to 826.746, P<0.001). Nomogram 2 was built based on tumor adjacent to the posterior thyroid capsule (95% CI: 2.922 to 53,074.51, P=0.017), distance <1 mm between tumor and the RLN (95% CI: 1.478 to 1,241.646, P=0.029), and loss of typical fascicular echotexture of the RLN along the long axis (95% CI: 35.11 to 53,272.81, P<0.001). In the validation cohort, nomogram 1 and 2 showed sensitivities of 94.74% and 57.89%, specificities of 74.12% and 95.29%, positive predictive values (PPV) of 45.00% and 73.26%, negative predictive values (NPV) of 98.43% and 91.03%, accuracies of 76.92% and 88.46%, and C-indices of 0.86 and 0.89.

Conclusions: Preoperative ultrasound is a feasible approach to evaluate RLN invasion in patients with thyroid carcinoma. Nomogram 1 may sensitively identify the risk of RLN invasion, and it may be checked using the more specific and accurate nomogram 2 to reduce false positives.

Keywords: Recurrent laryngeal nerve (RLN); invasion; thyroid carcinoma; ultrasonography; predictive model

Submitted Mar 15, 2023. Accepted for publication Aug 08, 2023. Published online Sep 11, 2023.
doi: 10.21037/qims-23-332
View this article at: https://dx.doi.org/10.21037/qims-23-332

Introduction

The global incidence of thyroid cancer has grown rapidly in the last 3 decades (1,2). Tumors in up to 20% of patients with thyroid cancer invade the recurrent laryngeal nerve (RLN) (3), which can cause nerve palsy manifesting as hoarseness or severe dyspnea (4,5). Such invasion disqualifies patients from robotic surgery, which is increasingly popular because it can lead to milder alterations of neck sensation and discomfort when swallowing than conventional thyroidectomy, while also avoiding scarring (6,7). Except low-risk well differentiated thyroid cancer (WDTC), patients with advanced/metastatic differentiated thyroid cancers (DTCs), anaplastic cancers, and medullary thyroid cancers (MTCs) are also increasing. These patients often present extrathyroidal extension (invasion of the vessels and nerves of the neck, trachea, esophagus, etc.), lymph node metastasis, and sometimes distant metastases (8). For resectable thyroid cancer, the American Thyroid Association (ATA) guidelines (9) require tumor staging with imaging before surgery, because evaluation of extent of local invasion may assist surgical decision-making. However, the current preoperative assessment methods are incomplete, especially for vessels and nerves.

Currently, RLN invasion before thyroidectomy is detected based on laryngoscopy by evaluating vocal cord mobility, but this approach is inadequate. First, vocal cord mobility may still be normal in the presence of unilateral lesions: some studies have reported that only about 30% of patients manifest vocal cord hypomobility during examination (10,11). Second, laryngoscopy is only an indirect indicator of RLN infiltration (12). These considerations highlight the need for a non-invasive way to predict RLN invasion when planning surgical treatment.

High-frequency ultrasonography is widely used to diagnose disorders involving peripheral nerves (13-17), and our previous study showed that preoperative ultrasound can be applied to visualize the RLN reliably (18). In our previous study, we injected the lymph nodes surrounding the RLN with carbon nanoparticles to confirm the same RLNs that had been identified by preoperative ultrasound during surgery. In addition, the concordance of results between preoperative and intraoperative ultrasound parameters [intraclass correlation coefficients (ICC) =0.403] and the statistics for measurements taken independently by 2 sonographers (ICCs ranged from 0.495 to 0.824) showed good reliability (Appendix 1, Method 1) (18). Therefore, we wondered whether preoperative ultrasonography could reliably detect RLN invasion in patients with thyroid carcinoma. In this study, we examined this question using independent patient cohorts at our hospital, leading to the establishment of 2 models that may help to identify those at high risk of RLN invasion in order to guide treatment decisions. We present this article in accordance with the STROBE reporting checklist (available at https://qims.amegroups.com/article/view/10.21037/qims-23-332/rc).

Methods

Patients

The study was conducted in accordance with the Declaration of Helsinki (as revised in 2013). The study was approved by the Ethics Committee of West China Hospital and informed consent was provided by all individual participants. This study was registered in the Chinese Clinical Trial Registry (ChinCTR2100049742). For development of a predictive model, a consecutive sample of patients who underwent thyroidectomy at the Department of Thyroid and Parathyroid Surgery Center at West China Hospital of Sichuan University between August 2020 and December 2021 were enrolled. To validate the model, a separate consecutive sample of patients between January 2022 and March 2022 was also enrolled (*Figure 1*).

To be randomly enrolled, patients had to meet the following criteria: (I) thyroid lesions detected by preoperative radiologic imaging, with or without enlargement of cervical lymph nodes; (II) undergo thyroid surgery, with pathology analysis of surgical specimens confirming thyroid carcinoma; (III) provide complete clinical information, including sex, age, height, weight, body mass index (BMI), and comorbidities; and (IV) undergo ultrasound evaluation of thyroid lesions and RLN within 1 week before surgery. Patients were excluded if they had a history of thyroidectomy, whether total or partial, or if surgical records or ultrasound imaging of RLN were incomplete or missing.

Ultrasonography

Thyroid lesion(s) and the RLN in each patient were analyzed by ultrasonography of the anterior cervical region as described (18), with the patient in the supine position and the neck at maximal extension (Appendix 1, Method 2). Longitudinal and transverse sections were captured with the thyroid lesions and RLN positioned in the middle of the

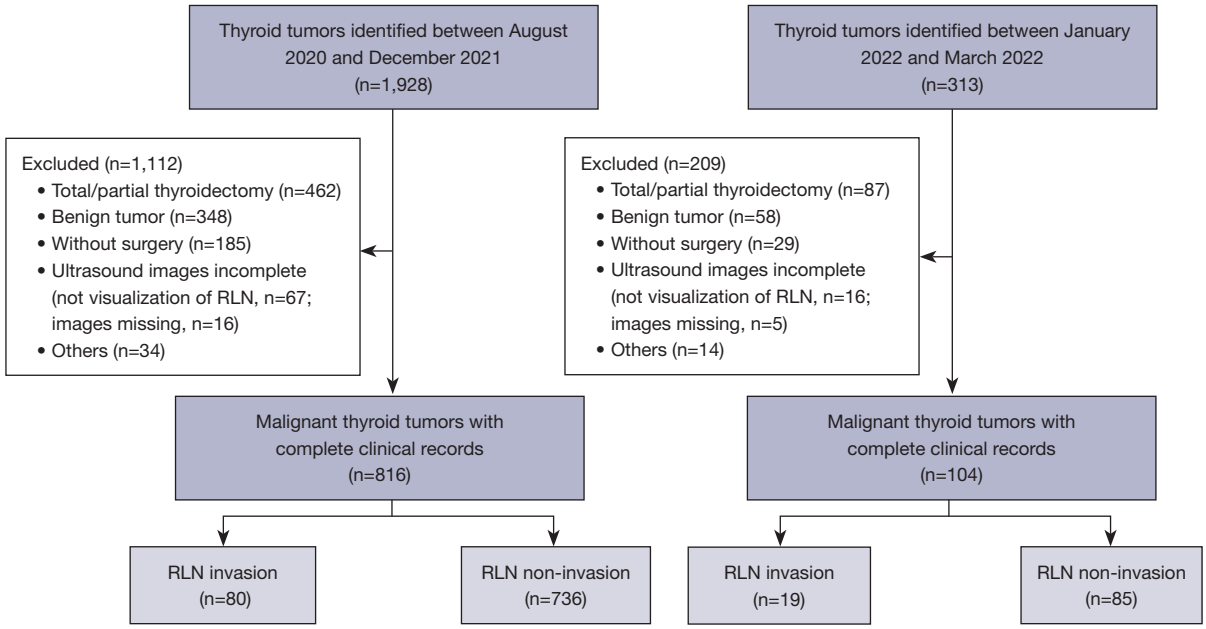

Figure 1 Flow diagram of patient inclusion in the development and validation cohorts. RLN, recurrent laryngeal nerve.

images. In this study, 2 ultrasound systems were used: an Aixplorer system (SuperSonic Imagine, Aix-en-Provence, France) with a 5–14 MHz line probe, and an RS80A system (Samsung Medison, Seoul, South Korea) with a 3–12 MHz linear probe.

Data were collected on the following imaging features: tumor location, categorized as diffuse, isthmic, upper, middle, or lower; tumor size; tumor margin, whether smooth or ill-defined; tumor shape, as regular or irregular; calcification, classified as macro, micro, mixed, or none; adjacency of the tumor to the anterior, posterior, medial, or lateral thyroid capsule; distance ≥1 or <1 mm between tumor and RLN; as well as loss of the typical fascicular echotexture of the RLN along the long axis, loss of the echotexture of the RLN epineurium, and loss of the echotexture of RLN fibers and perineurium, all categorized as yes or no. In patients with multiple lesions, we collected data only from the one that was categorized as 4b, 4c, or 5 according to Thyroid Imaging Reporting and Data System (TI-RADS) criteria (19,20) and that lay close to the tracheoesophageal groove.

Given that the RLN in healthy individuals resembles peripheral nerves in ultrasound images (typical fascicular echotexture appears as elongated structures with alternating hypo- and hyperechoic bands, *Figure 2A*,*2B*), we defined 2 ultrasound signs of RLN invasion (Appendix 1, Method 3; *Figure 2C*,*2D*): thyroid tumor <1 mm from the RLN (*Figure 2E*,*2F*), and loss of the typical fascicular echotexture of the RLN along the long axis (21,22).

Surgery and definitive diagnosis of RLN invasion

All surgeries were performed by 3 thyroid specialists using standard procedures (23,24) in 1 week (Appendix 1, Method 4). RLN invasion was detected by cryosections confirmation; alternatively, it was detected during the surgery itself in the following situations: (I) the tumor was found to adhere firmly to the RLN and electrical activity of the RLN was lost after resection, or resection also damaged the RLN; or (II) the RLN could not be preserved during surgery because it was intertwined with the tumor.

Statistical analysis

Data were analyzed using SPSS 19.0 (IBM Corp., Armonk, NY, USA) and R (v.3.3.3; R Foundation for Statistical Computing, Vienna, Austria). Continuous data were presented as the mean ± standard deviation. Inter-group differences in continuous data were assessed for significance using Student's *t*-test, whereas differences in categorical data were assessed using Pearson's chi-squared test. Variables that emerged as significantly associated with RLN invasion

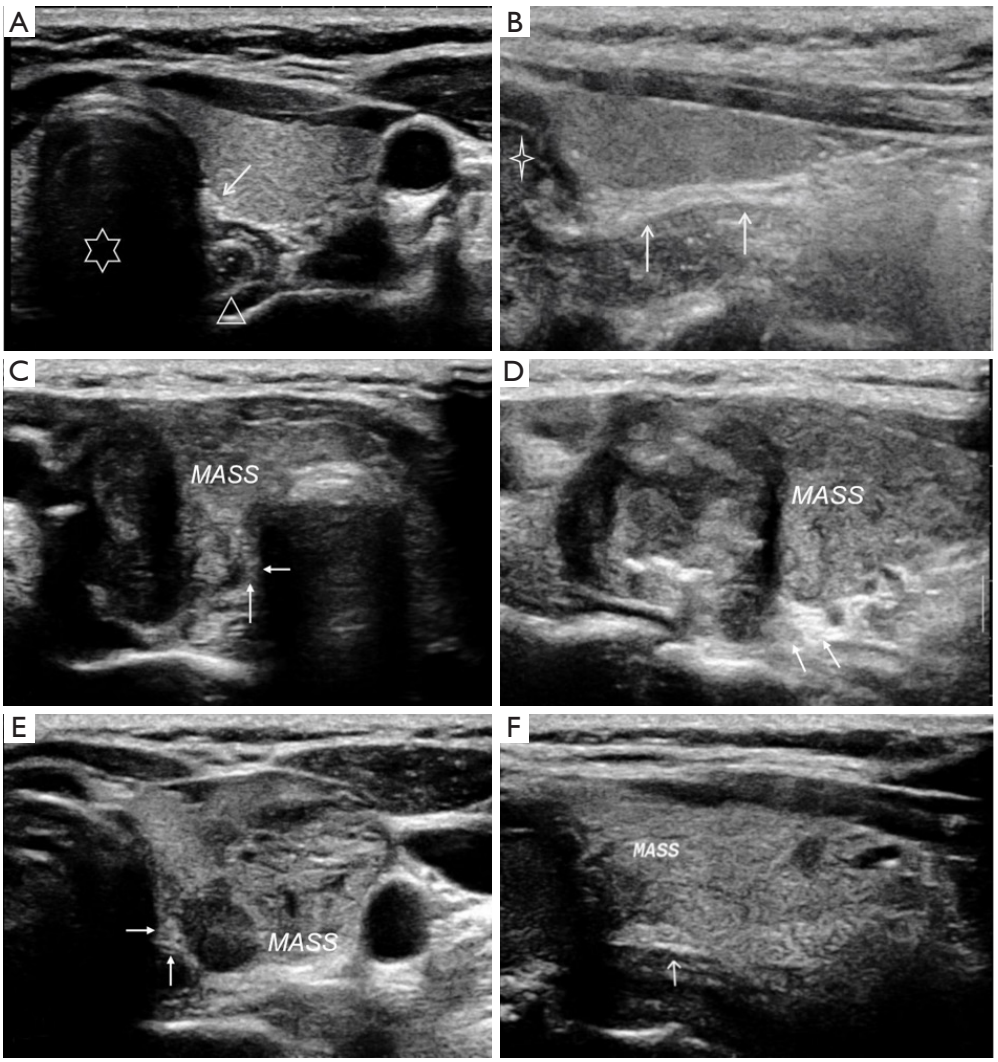

Figure 2 Examples of ultrasound images showing normal and invaded RLNs. (A) Image of a normal RLN along the short axis. (B) Image of a normal RLN along the long axis. (C) Image of an invaded RLN along the short axis. (D) Image of an invaded RLN along the long axis. (E) Image along the short axis of a tumor lying adjacent to the RLN without invading it. (F) tumor adjacent RLN without invasion along the long axis. Arrows indicate the RLN; the six-pointed star indicates the trachea; the triangle indicates the esophagus; the four-pointed star indicates cricoid cartilage; "MASS" indicates thyroid carcinoma. RLN, recurrent laryngeal nerve.

during univariate analysis were entered into multivariate logistic regression, and independent risk relationships were reported in terms of odds ratios (ORs) with 95% confidence intervals (CIs). Risk factors identified by multiple logistic regression were used to create predictive nomograms, for which cut-offs were determined using Youden's index. The ability of nomograms to diagnose RLN invasion was assessed in terms of sensitivity, specificity, positive predictive value (PPV) and negative predictive value (NPV), area under the receiver operating characteristic (ROC) curve (AUC), and concordance index (C-index). Results associated with $P<0.05$ (2-sided test) were considered statistically significant.

Results

Patient characteristics

Predictive nomograms were developed using data from 816 patients (612 women) whose mean age was 40±12 years,

and 80 of whom had RLN invasion. The frequent types of cancers were papillary carcinoma (769/816, 94.24%), medullary carcinoma (28/816, 3.43%), follicular carcinoma (8/816, 0.98%), anaplastic carcinoma (9/816, 1.10%), and squamous carcinoma (2/816, 0.25%). Most patients (614/816, 75.25%) had a single lesion, whereas fewer than 20% had Hashimoto's thyroiditis. According to the tumor-node-metastasis/American Joint Committee on Cancer (TNM/AJCC) classification, tumor staging was as follows: stage I (491/816, 60.17%), stage II (224/816, 27.45%), stage III (65/816, 7.97%), and stage IV (36/816, 4.41%).

The nomograms were validated in an independent cohort of 104 patients (85 women), whose mean age was 42±11 years and 19 of whom had RLN invasion. The distribution of types of thyroid carcinoma was similar to that in the cohort used to develop the nomograms.

Development of nomograms to predict RLN invasion

Univariate comparison of the clinicodemographic and ultrasound characteristics between patients with or without RLN invasion in the development cohort of 816 patients identified the following factors associated with invasion (Table S1): sex, age, BMI, lesion location, tumor size, calcification, tumor adjacent to any part of the thyroid capsule, distance between lesion and RLN, loss of typical fascicular echotexture of RLN along the long axis and loss of the echotexture of the RLN epineurium or fibers and perineurium. Forward stepwise multivariate regression with all these variables identified the following as independent predictors of invasion (*Table 1*): distance <1 mm between lesion and RLN, lesion adjacent to medial, posterior, and lateral thyroid capsules, tumor larger than 2 cm, age older than 60 years, and BMI ≥24 kg/m^2. The presence of high-risk features (distance <1 mm between lesion and RLN, lesion adjacent to medial and posterior thyroid capsules, tumor larger than 2 cm, age older than 60 years, BMI ≥24 kg/m^2 and loss of typical fascicular echotexture of RLN along the long axis) was associated with RLN invasion, and lower risk of invasion was observed with lesion adjacent to lateral thyroid capsule.

These 5 variables were incorporated into predictive nomogram 1, in which each variable was scored according to the ORs from multivariate logistic regression. As a result, score increased in larger lesion and older age. BMI ≥24 kg/m^2 was assigned a score of 29; distance <1 mm between lesion and RLN, 100; tumor adjacent to medial thyroid capsule, 43; and tumor adjacent to posterior thyroid capsule, 92. The total possible score ranged from 160 to 420, and Youden's index identified 260 as the ideal cut-off for predicting RLN invasion (*Figure 3A*).

Given that the nomogram 1 did not contain loss of typical fascicular echotexture of RLN along the long axis, which is widely applied in diagnosis of RLN invasion and recommended in several consensus guidelines (21,22), we decided to create nomogram 2 including this feature. Repeating multivariate logistic regression identified 3 independent risk factors of invasion (*Table 1*): loss of typical fascicular echotexture of RLN along the long axis, distance <1 mm between the tumor and RLN, and lesion adjacent to thyroid posterior capsule. The nomogram 2 with these 3 variables was defined as follows: [66 × tumor adjacent posterior capsule (no = 0, yes = 1)] + [59 × distance <1 mm (no = 0, yes = 1)] + [100 × loss of typical structure of RLN (no = 0, yes = 1)]. Youden's index identified 135 as the optimal cut-off (*Figure 3B*).

Calibration plots of both nomograms against the data from the development cohort of 816 patients showed good agreement between predicted and actual results (*Figure 3C,3D*). The C-index was 0.96 (95% CI: 0.94 to 0.98) for nomogram 1 and 0.99 (95% CI: 0.98 to 1.00) for nomogram 2. The corresponding AUCs were 0.89 (95% CI: 0.85 to 0.94) and 0.85 (95% CI: 0.77 to 0.92) (*Table 2*).

Nomogram validation

Both nomograms also performed well when we validated them against the second cohort of 104 patients. Nomogram 1 showed a C-index of 0.86 (95% CI: 0.78 to 0.94), AUC of 0.85 (95% CI: 0.77 to 0.91), and the following diagnostic performance indicators based on a cut-off of 260: sensitivity, 94.74%; specificity, 74.12%; PPV, 45.00%; NPV, 98.43%; and accuracy, 76.92% (*Table 3*). Nomogram 2 showed a C-index of 0.89 (95% CI: 0.80 to 0.97), AUC of 0.76 (95% CI: 0.33 to 0.79), and the following performance indicators based on a cut-off of 135: sensitivity, 57.89%; specificity, 95.29%; PPV, 73.26%; NPV, 91.03%; and accuracy, 88.46% (*Table 3*).

Discussion

Here we established 2 scoring models for predicting RLN invasion before surgery to treat thyroid carcinoma. Nomogram 1, which included clinicodemographic and ultrasound features, showed excellent sensitivity (94.74%) and NPV (98.43%). Nomogram 2, which included only

Table 1 Logistic regression to identify predictors of RLN invasion for two nomograms

Predictor (reference condition)	Category	Beta	OR (95% CI)	P
Nomogram 1				
Age (<30 years)	30 to <40	0.75	2.117 (0.334, 13.405)	0.426
	40 to <50	2.034	7.645 (0.819, 71.322)	0.074
	50 to <60	1.308	3.699 (0.451, 30.346)	0.223
	≥60	2.629	13.854 (1.315, 145.933)	0.029
Body mass index (<18.5 kg/m^2)	18.5 to <24	0.992	2.696 (0.395, 18.392)	0.311
	≥24	1.296	3.654 (1.228, 10.874)	0.020
Tumor size (≤10 mm)	>10–20	1.04	2.829 (0.712, 11.24)	0.140
	>20–40	1.903	6.708 (1.194, 37.685)	0.031
	>40	4.384	80.133 (4.677, 1,373.1)	0.002
Tumor adjacent to posterior thyroid capsule (no)	Yes	4.173	64.9 (5.567, 756.583)	0.001
Tumor adjacent to medial thyroid capsule (no)	Yes	1.941	6.965 (1.816, 26.713)	0.005
Tumor adjacent to lateral thyroid capsule	Yes	–2.353	0.095 (0.016, 0.559)	0.009
Distance <1 mm between tumor and RLN (no)	Yes	4.529	92.679 (10.389, 826.746)	<0.001
Nomogram 2				
Age (<30 years)	30 to <40	2.945	19.912 (0.505, 716.747)	0.112
	40 to <50	3.169	23.787 (0.486, 1,164.334)	0.110
	50 to <60	1.684	5.386 (0.119, 243.301)	0.386
	≥60	3.886	48.705 (0.634, 3,740.447)	0.079
Tumor size (≤10 mm)	>10–20	1.838	6.285 (0.366, 107.869)	0.205
	>20–40	0.408	1.504 (0.033, 69.515)	0.835
	>40	2.636	13.963 (0.113, 1,719.757)	0.283
Adjacent posterior thyroid capsule (no)	Yes	5.976	393.833 (2.922, 53,074.51)	0.017
Adjacent medial thyroid capsule (no)	Yes	2.006	7.437 (0.326, 169.512)	0.208
Adjacent lateral thyroid capsule (no)	Yes	–3.066	0.047 (0.0008, 2.581)	0.134
Distance between lesion and RLN (<1 mm) (no)	Yes	3.758	42.845 (1.478, 1,241.646)	0.029
Loss of the typical fascicular echotexture of RLN in long axis (no)	Yes	7.221	1,367.637 (35.11–53,272.81)	<0.001

RLN, recurrent laryngeal nerve; OR, odds ratio; CI, confidence interval.

ultrasound features, showed excellent specificity (95.29%) and accuracy (88.60%). Both models showed a C-index >0.86, suggesting good agreement with observations. Nomogram 1 may be useful for clinical screening because these features are relatively easy to obtain. Nomogram 2 may help refine clinical decision-making because of the added specificity of neurological ultrasound characteristics.

The variables in our sample that were significantly associated with RLN invasion overlapped with several of those identified in previous work (25), including older age, larger tumor, and tumor location near the posterior capsule. The differences in risk factors between that work and ours may reflect our larger RLN sample and the fact that, because of our focus on ultrasonography, we did not consider certain clinical features such as laryngoscopy.

Among the diverse variables that we examined, ultrasound features showed the strongest association with RLN invasion: the OR for distance <1 mm between tumor

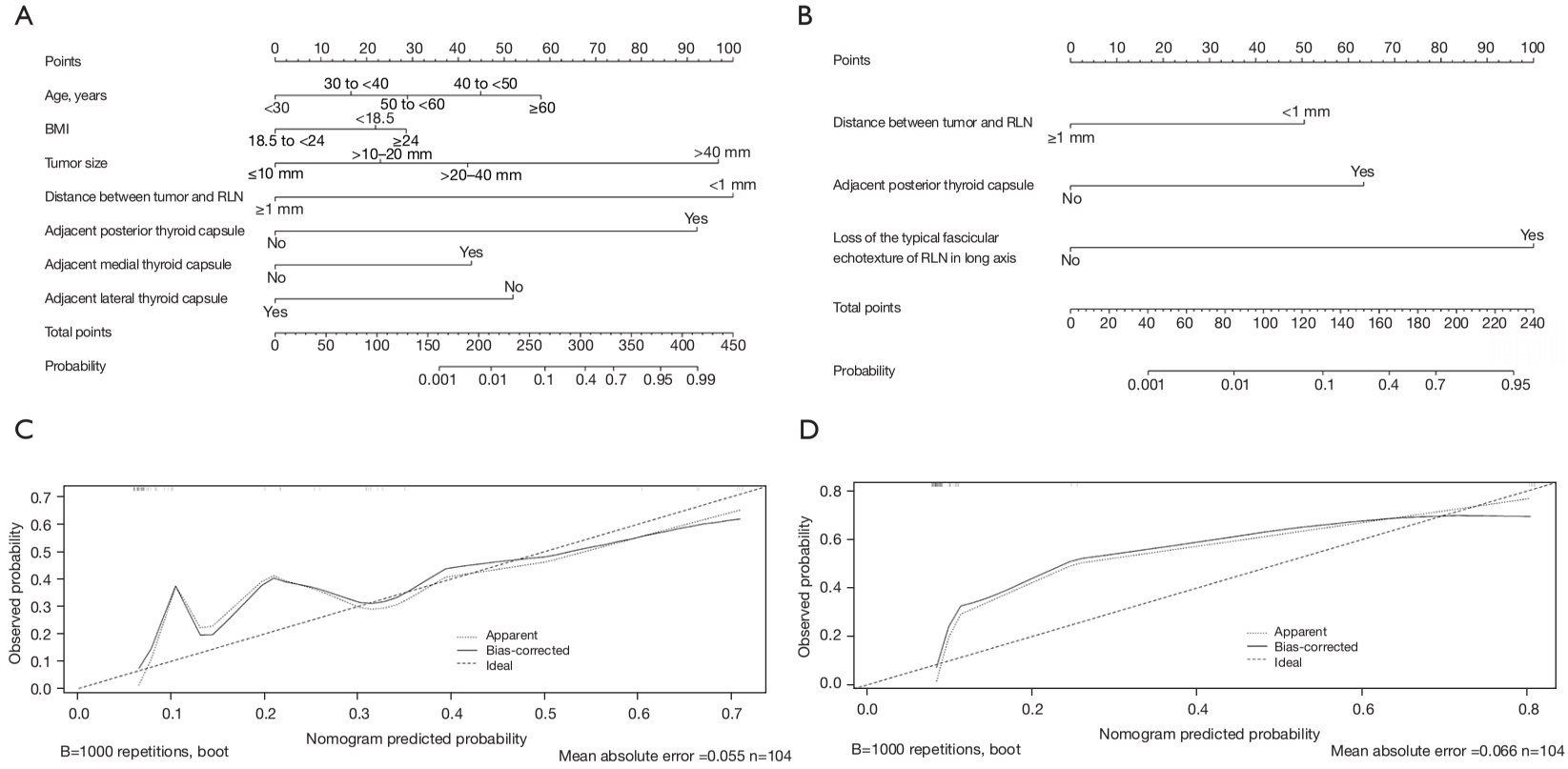

Figure 3 Nomograms and calibration curves for predicting RLN invasion. (A) Nomogram 1. (B) Nomogram 2. For both Nomograms, the linear predictor is the coordinate axis of the linear prediction value, and the linear prediction value is transformed into the corresponding probability value through a conversion function. (C) Calibration curves for Nomogram 1. (D) Calibration curves for Nomogram 2. Calibration curves, x-axis, and y-axis show the predicted probability and the actual ratios of recurrent laryngeal nerve invasion. The reference line is a dashed line that indicates the apparent calibration. BMI, body mass index; RLN, recurrent laryngeal nerve.

Table 2 Comparison of predictive performance in development and validation cohort

Models	C-index (95% CI)	AUC (95% CI)
Development cohort		
Nomogram 1	0.96 (0.94–0.98)	0.89 (0.85–0.94)
Nomogram 2	0.99 (0.98–1.00)	0.85 (0.77–0.92)
Validation cohort		
Nomogram 1	0.86 (0.78–0.94)	0.85 (0.77–0.91)
Nomogram 2	0.89 (0.80–0.97)	0.76 (0.33–0.79)

CI, confidence interval; AUC, area under curve.

Table 3 Performance of nomograms 1 and 2 in predicting RLN invasion in the validation cohort (n=104 patients)

Nomogram	Se, %	Sp, %	PPV, %	NPV, %	Accuracy, %
1	94.74	74.12	45.00	98.43	76.92
2	57.89	95.29	73.26	91.03	88.46

All values except the concordance index are %. RLN, recurrent laryngeal nerve; Se, sensitivity; Sp, specificity; PPV, positive predictive value; NPV, negative predictive value.

and RLN was 92.67 in nomogram 1, while the OR for loss of typical fascicular echotexture of the RLN was 1367.63 in nomogram 2. Our study provides the first comprehensive evidence that ultrasonography can be used to diagnose RLN invasion. Our results are consistent with previous work suggesting that among the most frequent ultrasound findings associated with invasion is the loss of fascicular echostructure (21,22,26). However, loss of fascicular echostructure correlates strongly with other factors from a statistical aspect in nomogram 1, which may explain why it was excluded from that model. To take into account the efficacy of ultrasonic features for diagnosis in previous research, we included loss of fascicular echostructure into nomogram 2, which proved to be more specific and accurate than nomogram 1.

Although both nomograms showed good diagnostic performance, they failed to detect RLN invasion in 8 patients in the validation cohort. There may be several reasons for this. One is that we relied on conventional ultrasonography, which does not provide coronal views, and the combination of transverse and sagittal sections can miss certain tumor features (27,28). In 3 patients, we diagnosed RLN infiltration on the basis of loss of typical fascicular echotexture along the long axis, yet invasion was not detected in any of the 3 patients during surgery. We might have correctly determined no invasion from ultrasound images if we had visualized the entire RLN in a coronal image. Other contributors to missed diagnoses may include macro calcification and peripheral calcification, acoustic shadows caused by calcification, as well as architectural distortions that blur the margin between tumor and RLN.

There are some limitations in our study. First, RLN invaded by metastatic central cervical lymph nodes was not discussed in this study. There were 12 cases with RLN invaded by metastatic central cervical lymph nodes that ultrasound failed to detect due to the lack of background parenchymal contrast below thyroid and hyperechoic of the surrounding connective tissues. The characteristics of infiltrated RLN could not be analyzed because of the limited sample (29). Second, we excluded patients in whom ultrasonography failed to visualize the RLN clearly, which may have biased our development and validation cohorts. Third, the percentage of patients with advanced thyroid carcinoma was relatively higher in our institution, which may contribute to a higher incidence of RLN invasion (10%) in this trail. Fourth, this was a single-center prospective analysis, as this design conducted a new method for evaluating RLN invasion in thyroid carcinoma. Our data was derived from a single institution; the generalizability can be improved if data from additional institutions is added to the training set. Our research supplied more information of RLNs to help surgeons evaluate the surgical options for patients with resectable thyroid cancer. Patients with advanced/metastatic DTCs, anaplastic cancers, and

MTCs who had the rare opportunity to receive surgery treatment after assessment of local invasion might accept multidisciplinary options including primary chemoradiation, palliative radiotherapy, and systemic therapy as early as possible to approach a better supportive care.

Conclusions

Our work indicates that preoperative ultrasound is a feasible approach to evaluate RLN invasion in patients with thyroid carcinoma. We developed nomogram 1 that may be useful for easy, rapid screening of patients for risk of invasion. The results from nomogram 1 can be refined using nomogram 2, which is more specific and accurate yet requires skillful interpretation of neck anatomy in ultrasound images. These findings suggest that preoperative ultrasound evaluation of RLN could supply additional information for individual surgical treatment decision.

Acknowledgments

Funding: None.

Footnote

Reporting Checklist: The authors have completed the STROBE reporting checklist. Available at https://qims.amegroups.com/article/view/10.21037/qims-23-332/rc

Conflicts of Interest: All authors have completed the ICMJE uniform disclosure form (available at https://qims.amegroups.com/article/view/10.21037/qims-23-332/coif). The authors have no conflicts of interest to declare.

Ethical Statement: The authors are accountable for all aspects of the work in ensuring that questions related to the accuracy or integrity of any part of the work are appropriately investigated and resolved. The study was conducted in accordance with the Declaration of Helsinki (as revised in 2013). The study was approved by the Ethics Committee of West China Hospital and informed consent was provided by all individual participants.

References

1. Kim JI, Kim SJ, Xu Z, Kwak J, Ahn JH, Yu HW, Chai YJ, Choi JY, Lee KE. Efficacy of Intraoperative Neuromonitoring in Reoperation for Recurrent Thyroid Cancer Patients. Endocrinol Metab (Seoul) 2020;35:918-24.
2. Sung H, Ferlay J, Siegel RL, Laversanne M, Soerjomataram I, Jemal A, Bray F. Global Cancer Statistics 2020: GLOBOCAN Estimates of Incidence and Mortality Worldwide for 36 Cancers in 185 Countries. CA Cancer J Clin 2021;71:209-49.
3. Chiang FY, Wang LF, Huang YF, Lee KW, Kuo WR. Recurrent laryngeal nerve palsy after thyroidectomy with routine identification of the recurrent laryngeal nerve. Surgery 2005;137:342-7.
4. Jeannon JP, Orabi AA, Bruch GA, Abdalsalam HA, Simo R. Diagnosis of recurrent laryngeal nerve palsy after thyroidectomy: a systematic review. Int J Clin Pract 2009;63:624-9.
5. Erbil Y, Barbaros U, Işsever H, Borucu I, Salmaslioğlu A, Mete O, Bozbora A, Ozarmağan S. Predictive factors for recurrent laryngeal nerve palsy and hypoparathyroidism after thyroid surgery. Clin Otolaryngol 2007;32:32-7.
6. Lee J, Chung WY. Robotic surgery for thyroid disease. Eur Thyroid J 2013;2:93-101.
7. Lee J, Yun JH, Nam KH, Choi UJ, Chung WY, Soh EY. Perioperative clinical outcomes after robotic thyroidectomy for thyroid carcinoma: a multicenter study. Surg Endosc 2011;25:906-12.
8. Laha D, Nilubol N, Boufraqech M. New Therapies for Advanced Thyroid Cancer. Front Endocrinol (Lausanne) 2020;11:82.
9. Bible KC, Kebebew E, Brierley J, Brito JP, Cabanillas ME, Clark TJ Jr, Di Cristofano A, Foote R, Giordano T, Kasperbauer J, Newbold K, Nikiforov YE, Randolph G, Rosenthal MS, Sawka AM, Shah M, Shaha A, Smallridge R, Wong-Clark CK. 2021 American Thyroid Association Guidelines for Management of Patients with Anaplastic Thyroid Cancer. Thyroid 2021;31:337-86.
10. Rosato L, Carlevato MT, De Toma G, Avenia N. Recurrent laryngeal nerve damage and phonetic modifications after total thyroidectomy: surgical

malpractice only or predictable sequence? World J Surg 2005;29:780-4.
11. Kay-Rivest E, Mitmaker E, Payne RJ, Hier MP, Mlynarek AM, Young J, Forest VI. Preoperative vocal cord paralysis and its association with malignant thyroid disease and other pathological features. J Otolaryngol Head Neck Surg 2015;44:35.
12. Dionigi G, Boni L, Rovera F, Rausei S, Castelnuovo P, Dionigi R. Postoperative laryngoscopy in thyroid surgery: proper timing to detect recurrent laryngeal nerve injury. Langenbecks Arch Surg 2010;395:327-31.
13. Abraham A, Izenberg A, Dodig D, Bril V, Breiner A. Peripheral Nerve Ultrasound Imaging Shows Enlargement of Peripheral Nerves Outside the Brachial Plexus in Neuralgic Amyotrophy. J Clin Neurophysiol 2016;33:e31-3.
14. Samarawickrama D, Therimadasamy AK, Chan YC, Vijayan J, Wilder-Smith EP. Nerve ultrasound in electrophysiologically verified tarsal tunnel syndrome. Muscle Nerve 2016;53:906-12.
15. Gruber H, Glodny B, Bendix N, Tzankov A, Peer S. High-resolution ultrasound of peripheral neurogenic tumors. Eur Radiol 2007;17:2880-8.
16. Goedee HS, Brekelmans GJ, van Asseldonk JT, Beekman R, Mess WH, Visser LH. High resolution sonography in the evaluation of the peripheral nervous system in polyneuropathy--a review of the literature. Eur J Neurol 2013;20:1342-51.
17. Huang A, Jiang L, Zhang J, Wang Q. Attention-VGG16-UNet: a novel deep learning approach for automatic segmentation of the median nerve in ultrasound images. Quant Imaging Med Surg 2022;12:3138-50.
18. He Y, Li Z, Yang Y, Lei J, Peng Y. Preoperative Visualized Ultrasound Assessment of the Recurrent Laryngeal Nerve in Thyroid Cancer Surgery: Reliability and Risk Features by Imaging. Cancer Manag Res 2021;13:7057-66.
19. Zhou J, Yin L, Wei X, Zhang S, Song Y, Luo B, et al. 2020 Chinese guidelines for ultrasound malignancy risk stratification of thyroid nodules: the C-TIRADS. Endocrine 2020;70:256-79.
20. Liang F, Li X, Ji Q, He D, Yang M, Xu Z. Revised Thyroid Imaging Reporting and Data System (TIRADS): imitating the American College of Radiology TIRADS, a single-center retrospective study. Quant Imaging Med Surg 2023;13:3862-72.
21. Kerasnoudis A, Tsivgoulis G. Nerve Ultrasound in Peripheral Neuropathies: A Review. J Neuroimaging 2015;25:528-38.
22. Telleman JA, Herraets IJ, Goedee HS, van Asseldonk JT, Visser LH. Ultrasound scanning in the diagnosis of peripheral neuropathies. Pract Neurol 2021;21:186-95.
23. Gao M, Ge M, Ji Q, Cheng R, Lu H, Guan H, et al. 2016 Chinese expert consensus and guidelines for the diagnosis and treatment of papillary thyroid microcarcinoma. Cancer Biol Med 2017;14:203-11.
24. Haugen BR, Alexander EK, Bible KC, Doherty GM, Mandel SJ, Nikiforov YE, Pacini F, Randolph GW, Sawka AM, Schlumberger M, Schuff KG, Sherman SI, Sosa JA, Steward DL, Tuttle RM, Wartofsky L. 2015 American Thyroid Association Management Guidelines for Adult Patients with Thyroid Nodules and Differentiated Thyroid Cancer: The American Thyroid Association Guidelines Task Force on Thyroid Nodules and Differentiated Thyroid Cancer. Thyroid 2016;26:1-133.
25. Chen W, Lei J, You J, Lei Y, Li Z, Gong R, Tang H, Zhu J. Predictive factors and prognosis for recurrent laryngeal nerve invasion in papillary thyroid carcinoma. Onco Targets Ther 2017;10:4485-91.
26. Beekman R, Visser LH. High-resolution sonography of the peripheral nervous system -- a review of the literature. Eur J Neurol 2004;11:305-14.
27. Tang G, An X, Xiang H, Liu L, Li A, Lin X. Automated Breast Ultrasound: Interobserver Agreement, Diagnostic Value, and Associated Clinical Factors of Coronal-Plane Image Features. Korean J Radiol 2020;21:550-60.
28. Timor-Tritsch IE, Monteagudo A, Ramos J, Kupchinska S, Mastriciani F, Spier M. Three-Dimensional Coronal Plane of the Uterus: A Critical View for Diagnostic Accuracy. J Ultrasound Med 2021;40:607-19.
29. Xing Z, Qiu Y, Yang Q, Yu Y, Liu J, Fei Y, Su A, Zhu J. Thyroid cancer neck lymph nodes metastasis: Meta-analysis of US and CT diagnosis. Eur J Radiol 2020;129:109103.

Cite this article as: He Y, Yang Y, Wen W, Qiu L, Li Z, Lei J. Predicting recurrent laryngeal nerve invasion by preoperative ultrasonography in patients with thyroid carcinoma. Quant Imaging Med Surg 2023;13(10):7002-7011. doi: 10.21037/qims-23-332

Appendix 1

Supplementary methods

Method 1: identification and visualization of RLN by ultrasound

Due to dehydration and tissue degeneration of the cadaver, we could not confirm the RLN on the necropsy autopsy. Additionally, as it impossible to label RLN directly on patients, we used the following two solutions:

(I) Carbon nanoparticle injection: we selected 1 lymph node adjacent to the RLN in patients for injection of 0.1 mL carbon nanoparticles (Lai Mei Pharmaceutical Co., Chongqing, China) and the interval time from injection to surgery was less than 24 hours. The marked lymph nodes, recognized during surgery, proved to be adjacent to the RLN identified by preoperative ultrasound, as expected.

(II) Repeatability of RLN visualization: pre- and intra-operative measurements, intra- and inter-observer measurements were assessed using single-measure intraclass correlation coefficients (ICC). The concordance of results between preoperative and intraoperative ultrasound parameters was moderate (ICC 0.403). The ICCs for measurements taken independently by 2 ultrasonographers ranged from 0.495 to 0.824.

Method 2: preoperative ultrasound examination of the RLN

The ultrasound probe was placed at the paratracheal area, perpendicular to the coronal body plane. The operator started to scan the RLNs which were identified with the transducer in a transverse position, and color Doppler mode was used to distinguish the RLNs from small blood vessels. From this position, the nerve was tracked upwards to the entry of the laryngeal area and downwards to the supraclavicular area, with slight adjustments of the scanning plane. Finally, the ultrasound transducer was rotated into a longitudinal position with respect to the long axis in order to further identify thyroid lesions and the RLNs. The same steps were performed on the other side.

Method 3: appearance of normal nerves in ultrasound images

Normal peripheral nerves show a "honeycomb-like" appearance along the short axis, related to the presence of hypoechoic axons arranged in fascicles and multiple layers of hyperechoic connective tissue surrounding the axon bundles. The nerve appears as an elongated structure along the long axis, with alternating hypo- and hyper-echoic bands.

Method 4: exposure of the RLN during surgery

The borders of the exposed RLN were as follows: upper, the laryngeal entry point; lower, the innominate artery; medial, the trachea; and lateral, the inner edge of the common carotid artery.

https://dx.doi.org/10.21037/qims-23-332

Table S1 Univariate analysis to identify factors associated with RLN invasion

Factor	Category	No RLN invasion (n=736)	RLN invasion (n=80)	P value
Sex	Male	176 (75.00)	28 (25.00)	0.041
	Female	560 (85.64)	52 (14.36)	
Age, years	<30	132 (90.12)	8 (9.88)	<0.001
	30 to <40	279 (88.24)	20 (11.76)	
	40 to <50	155 (83.51)	16 (16.49)	
	50 to <60	118 (82.67)	13 (17.33)	
	≥60	52 (54.9)	23 (45.1)	
Body mass index, kg/m^2	<18.5	59 (82.05)	7 (17.95)	0.008
	18.5 to <24	449 (87.18)	35 (12.82)	
	≥24	228 (76.54)	38 (23.46)	
Tumor location	Diffuse	30 (54.54)	22 (45.46)	<0.001
	Isthmic	22 (100.00)	0 (0.00)	
	Upper	118 (95.16)	6 (4.84)	
	Middle	338 (89.65)	39 (10.35)	
	Lower	228 (94.61)	13 (5.39)	
Tumor size, mm	≤10	442 (93.68)	16 (6.32)	<0.001
	>10–20	184 (79.03)	26 (20.97)	
	>20–40	88 (70.59)	20 (29.41)	
	>40	22 (37.93)	18 (62.07)	
Tumor margin	Smooth	37 (91.30)	2 (8.70)	0.417
	Ill-defined	669 (82.71)	78 (17.29)	
Tumor shape	Regular	37 (95.45)	1 (4.55)	0.125
	Irregular	699 (82.52)	79 (17.48)	
Calcification	Macro	22 (71.43)	4 (38.57)	0.025
	Micro	441 (86.81)	36 (13.19)	
	Mixed	206 (76.35)	35 (23.65)	
	None	67 (87.18)	5 (12.82)	
Tumor adjacent to anterior thyroid capsule	Yes	236 (77.58)	37 (22.42)	0.013
	No	500 (98.13)	4 (1.87)	
Tumor adjacent to posterior thyroid capsule	Yes	346 (70.77)	76 (29.23)	<0.001
	No	390 (98.13)	4 (1.87)	
Tumor adjacent to medial thyroid capsule	Yes	213 (68.45)	53 (31.55)	<0.001
	No	523 (91.18)	27 (8.82)	
Tumor adjacent to lateral thyroid capsule	Yes	177 (70.9)	39 (29.1)	<0.001
	No	559 (87.94)	41 (12.06)	
Distance <1 mm between tumor and RLN	Yes	206 (58.64)	79 (41.36)	<0.001
	No	530 (99.65)	1 (0.35)	
Loss of typical fascicular echotexture of the RLN	Yes	29 (17.89)	78 (82.11)	<0.001
	No	707 (99.47)	2 (0.53)	
Loss of the echotexture of RLN epineurium	No	707 (99.47)	2 (0.53)	<0.001
	Yes	29 (17.89)	78 (82.11)	
Loss of the echotexture of RLN fibers and perineurium	Yes	8 (1.47)	67 (98.53)	<0.001
	No	728 (96.80)	13 (3.20)	

Values are n (%), unless otherwise indicated. RLN, recurrent laryngeal nerve.

https://dx.doi.org/10.21037/qims-23-332